

Sea of Japan

Arnold L. Gordon
 Lamont-Doherty Geological Observatory
 Columbia University
 Palisades, New York, 10964

AD-A226 309

1990

ONR

DTIC
ELECTE
SEP 07 1990
S DCS D

Summary-

The Sea of Japan (Fig. 1) represents a unique oceanic environment that offers the possibility for quantitative sea-air exchange research of a 'thermohaline' active region. For the Sea of Japan the heat and salinity budgets can be addressed by: (1) monitoring ocean current inflow/outflow thermohaline and volume flux characteristics; (2) using the ring of meteorological coastal stations for monitoring atmospheric marine boundary layer changes during transit of the Sea of Japan; (3) following the standard sea surface & lower atmosphere vertical gradients methods with ship data. Each provides a check on the other allowing a pretty well resolved environment. An important consequence of Sea of Japan research may be the refinement of our methods of determining sea-air fluxes from ship data. Other benefit related to vertical mixing in the ocean interior may also be realized. ←

Figure 2 presents in schematic form many of the issues that are mentioned in the Summary, below.

The Tsushima Current injects $3 \text{ to } 5 \times 10^6 \text{ m}^3\text{sec}^{-1}$ of the warm-salty Kuroshio water into the Sea of Japan via the narrow straits between Japan and Korea, sill depth of mostly 150 meters, but with a narrow channel at 200 meters. Monitoring of the Tsushima Current (Fig. 3a, b) has been done with current meters and geostrophic approximation (that may not be too good for the confined shallow Korean Strait). Bottom moored ADCP might be a better way for future monitoring of the velocity profile; submarine telephone cables might be useful for transport monitoring. Tsushima water once in the deep semi-enclosed sea is exposed to extreme winter air masses flowing off the Asian continent (Fig. 4) which converts it to colder, less salty water masses that eventually find their way out of the Sea through two northern passages: Tsugaru Current advecting $3 \times 10^6 \text{ m}^3\text{sec}^{-1}$; over a 200 meter sill depth and the Soya Current carrying $1 \times 10^6 \text{ m}^3\text{sec}^{-1}$, with a 50 meter sill depth. A schematic of the flow

patterns is given in Fig. 5. Using temperature and current information at all three controlling straits (Fig. 6) suggests a annual loss of heat within the Sea of Japan of 40 wm^{-2} .

The waters masses form at two sites: near the USSR margins where bottom water is formed and along a frontal zone, referred to as the Polar Front, separating the southern warm regime from the northern cold regime (Fig. 2 & its insert) where intermediate water is formed. Rapid surveys with XBT and inspection of satellite derived infra-red images reveal that the Polar Front is much more variable than the climatic picture (Fig. 7). Large meanders and eddies associated with the front can support significant lateral eddies fluxes required to balance the sea water buoyancy loss west and north of the polar front. Pools of warm-salty water, derived from the Tsushima Current, flowing along the southeast boundary of the Sea of Japan may migrate toward the northwest into the cold regime. Exposure to cold air induces modifications form the intermediate water (stratum of low salinity; high oxygen) that spreads near the sill depth of 150-250 meters (Fig. 8).

The bottom water ventilates the sea floor of the Japan Basin. Newly formed bottom water then spreads to the Yamoto Basin in the southern Sea of Japan across a 2300 meter connecting (Fig. 9 & 10). Between 150 meter controlling sill depth and the bottom water the Sea of Japan θ/S relation suggest that the balance is primarily along the vertical coordinate. Assuming a K_z of 1 cgs unit yields a bottom water production rate of only $0.05 \times 10^6 \text{ m}^3\text{sec}^{-1}$, residence time of 380 years. Since K_z is probably larger (considering the confined sea with a large wall area to interior volume ratio and moderate tidal oscillation and the low static stability of the sub-sill water column); with a K_z of 10 cgs the production rate goes up one order: $0.5 \times 10^6 \text{ m}^3\text{sec}^{-1}$ residence time of 38 years. This seems more 'intuitively correct'.

The use of tracers distribution, particularly CFCs within the Sea of Japan would resolved the ventilation rate and allow estimates of K_z within the 1-D 150 to 3700 meters slab of the Sea of Japan. This is yet another unique and useful attribute of the Sea of Japan.

Modified water of the Sea of Japan can escape into the open Pacific Ocean with the Tsugaru Current. The Tsugaru Passage with a 200 meter sill depth can release the intermediate water formed within the Sea. Studies reveal that the Tsugaru Current can be

page 2

STATEMENT "A" per Alan Brandt
 ONR. Code 1121SS
 TELECON 9/5/90 VG

Dist	and/or special
A-1	



<input checked="" type="checkbox"/>
<input type="checkbox"/>
<input type="checkbox"/>
by Codes
per call

monitored very well by monitoring sea level slope across and along the Strait. Once into the Pacific the Tsugaru water curls toward the south and forms a ribbon along the northern edge of the Kuroshio Current. Might the Sea of Japan play a role in the ventilation of the western Pacific?

For the Sea of Japan the ocean/atmosphere exchanges can be studied from meteorological measurements. This approach provides an independent estimation of thermohaline fluxes. Meteorological stations along the USSR coast and those along the Japanese coast can be used to measure the modification to the heat and water vapor content of the marine boundary layer as it sweeps across the Sea of Japan. This provides information on the heat and water exchanges across the sea-air interface. This has been done for air masses flowing off southeast US and in the Southern Ocean. In these cases the initial air column characteristics are defined by coastal stations but at sea air column was measured by ships. In the Sea of Japan the ring of met stations allows for more continuous study of the evolution of the marine boundary layer (for winter air masses spreading to the southeast and for summer air masses spreading into the Asian continent) and may be an effective method to obtain sea-air fluxes.

Study of the Tsushima Current and deep water characteristics reveal the presence of variability. Are these linked? Might increase in the inflow of warm-salty Kuroshio water increase the sea-air fluxes and reduce residence times, a more vigorous water mass modification rate? Or do changes in deep and bottom water characteristics simply reflect the severity of the local winter.

List of Key Science Issues of the Sea of Japan-

- **Heat/Salinity Budgets:**
 - Inflow/Outflow Constraint**
 - Atmospheric Boundary Layer modification**
 - Sea-Air Fluxes Determinations**

- **Formation/Residence Times of Sea of Japan Water Mass**
 - Intermediate Water**
 - Deep & Bottom Water**

- **Relation of Temporal Variations of Water Mass Formation To**
 - Inflow mass and heat/salinity flux**
 - Coldness of the winter**

Figures-

Figure 1- Sea of Japan bathymeter: average depth 3700 meters; area: $0.7 \times 10^6 \text{ km}^2$; volume: $2 \times 10^6 \text{ km}^3$.

Figure 2- Schematic of various thermohaline processes within the Sea of Japan.

Figure 3- Tsushima Current velocity field and transport. Note stronger flow plus more shear during summer.

Figure 4- Winter and summer air temperatures and sea surface temperatures. In winter the climatic air temperature in the northwest edge of the Sea is as much as 10°C below the water temperature, drawing lots of heat from the ocean forming denser water which sinks to the sea floor, ventilating the sub-sill volume of the Sea of Japan.

Figure 5- Sea of Japan circulation pattern.

Figure 6- Temperature sections across each of the three main passage connecting the Sea of Japan with the open Pacific Ocean.

Figure 7- Climatic and synoptic temperature patterns within the Sea of Japan.

Figure 8- Temperature and salinity sections across the eastern side of the Sea of Japan. The shallow warm-salty inflow and intermediate water stratum float above the nearly homogeneous deep and bottom water.

Figure 9- Schematic of the bottom water formation pattern of the Sea of Japan.

Figure 10- Temperature and oxygen profiles in the deep and bottom waters of the Sea of Japan. From the salinity minimum intermediate water stratum near 150 to 200 meters; the θ/S is essentially a straight line indication simply advective-diffusion balance along the vertical coordinate.

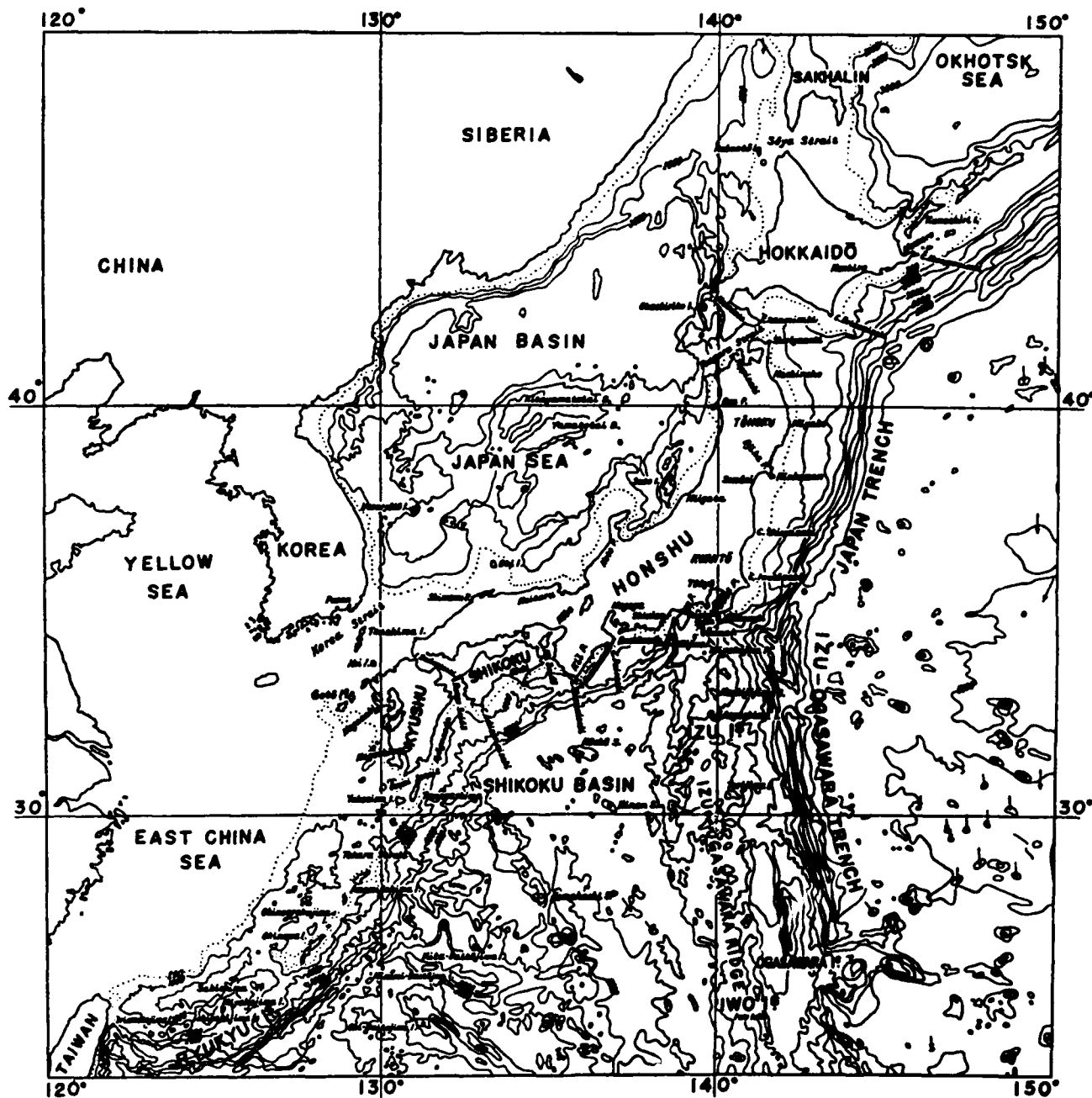


FIG. 1 Bathymetry and geographical names of the adjacent seas of the Japanese Islands. Compiled from J.H.O. chart No. 6301 and 6302.

Fig. 1

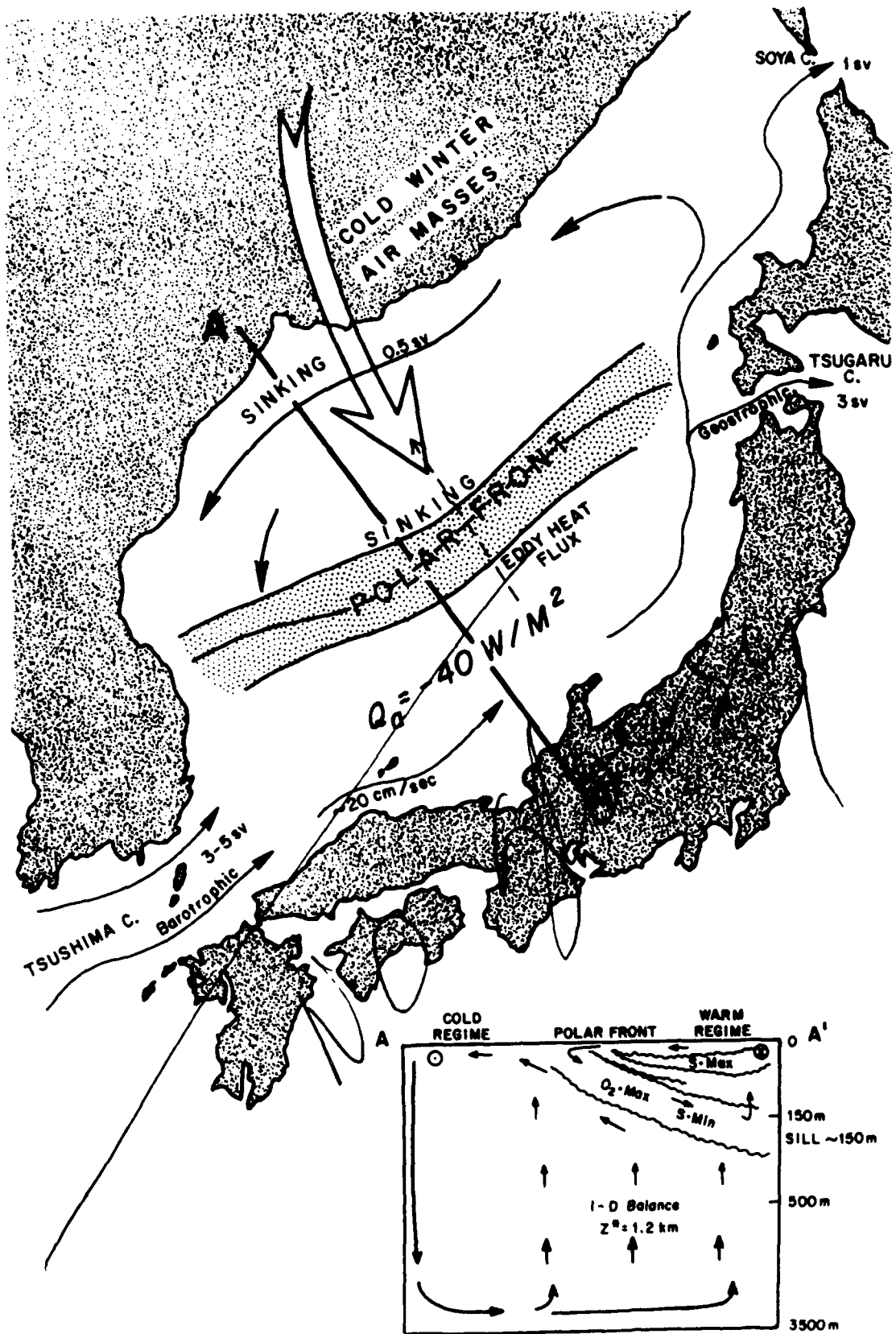


Fig. 2

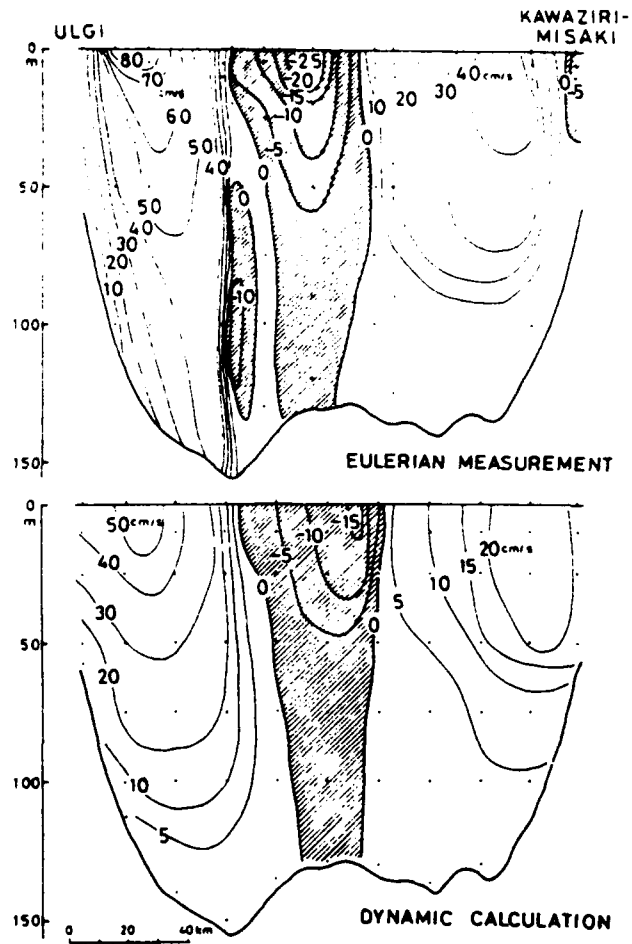


Fig. 3a

Fig. 3. Distribution of speed at section I. (a) Eulerian measurement. (b) Dynamic calculation.

Fig. 3b

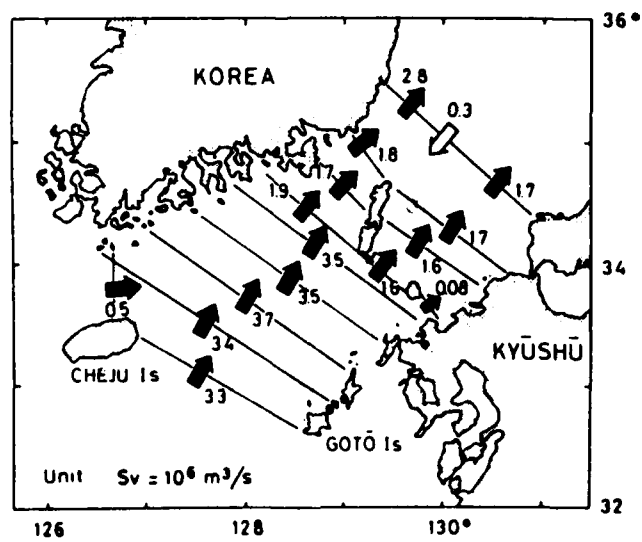


Fig. 4. Volume transport.

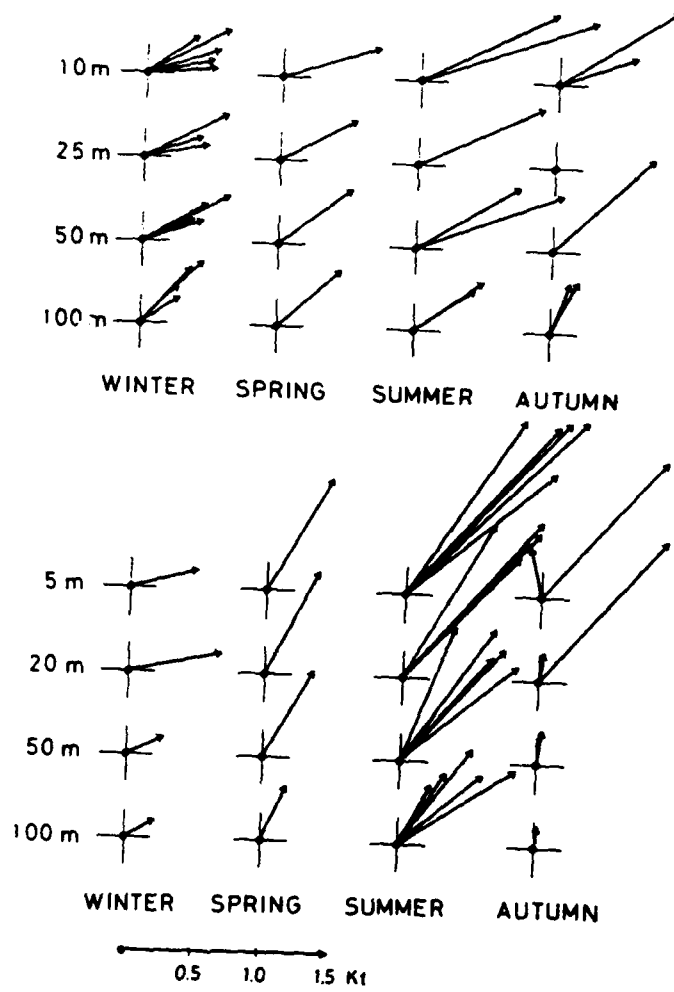


Fig. 5. Seasonal change of current vectors.

Fig. 3c

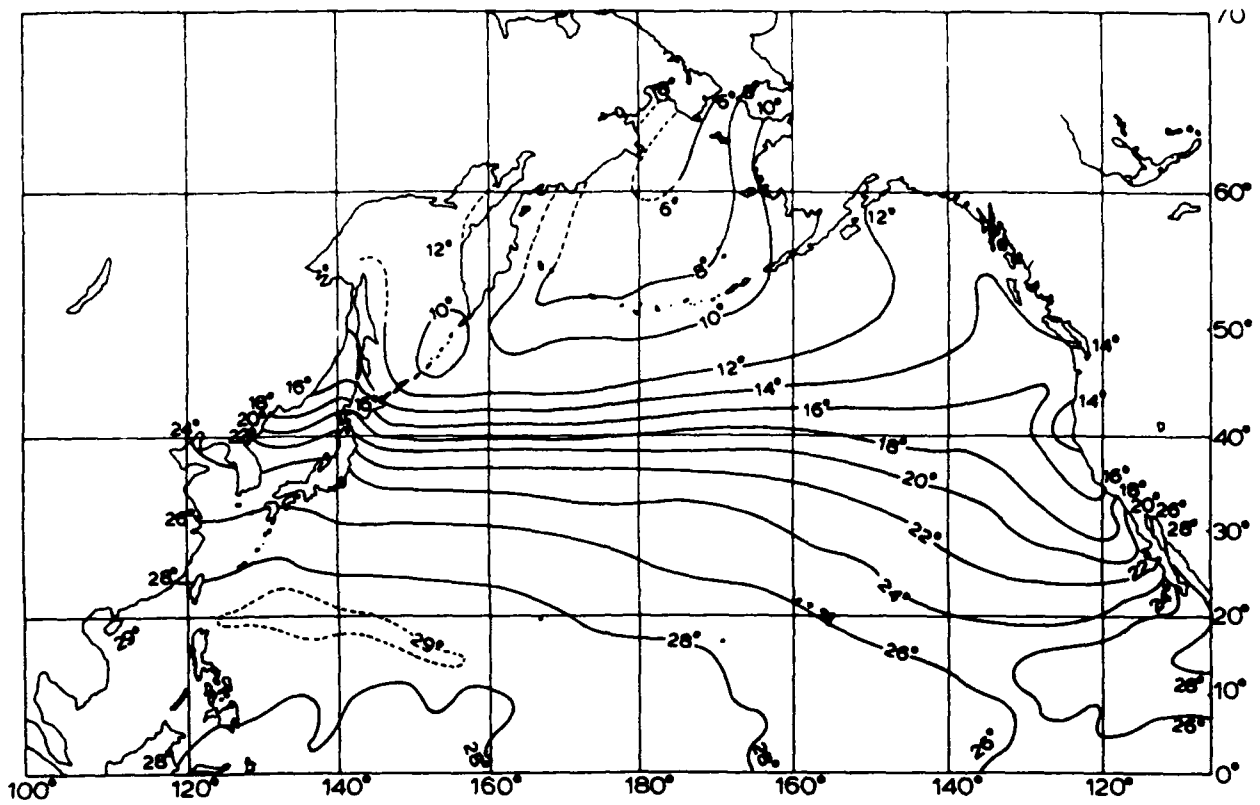


Fig. 20. Air temperature, July.

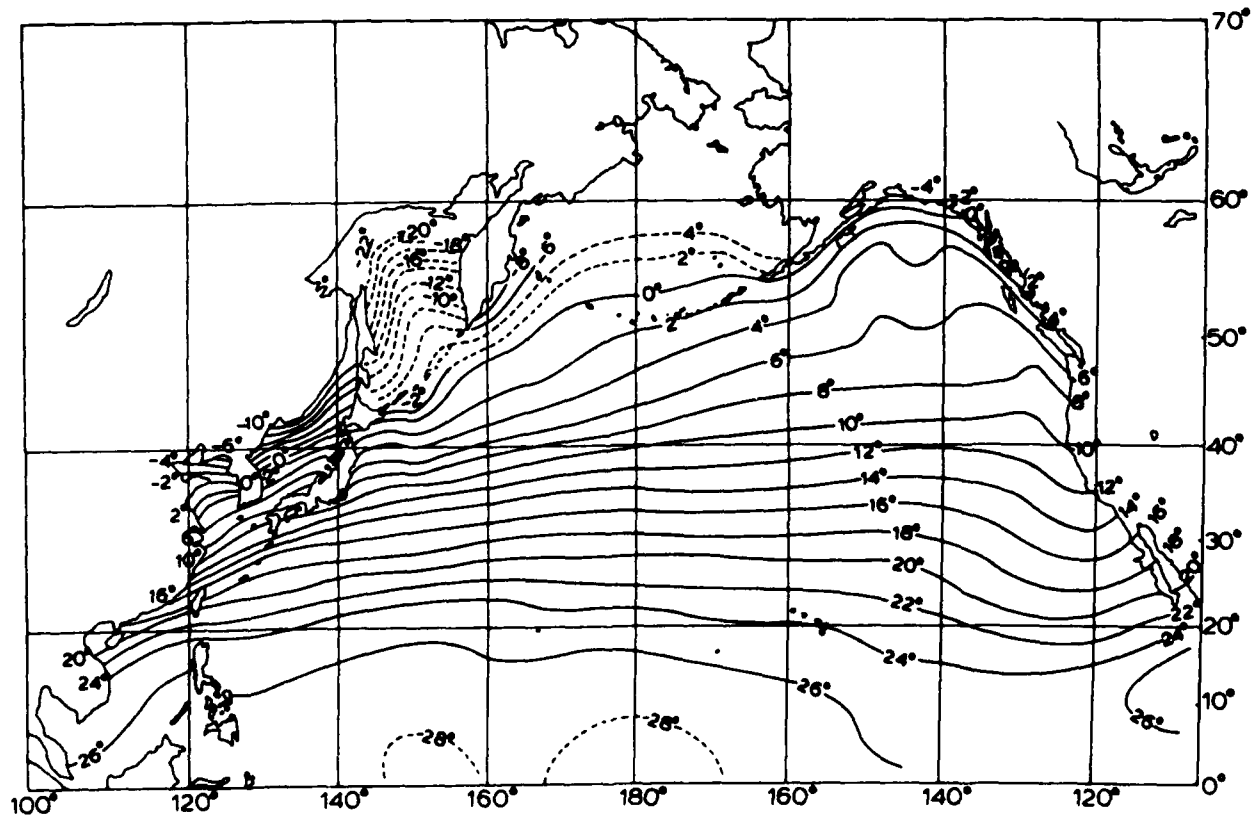


Fig. 21. Air temperature, January

Fig. 4a

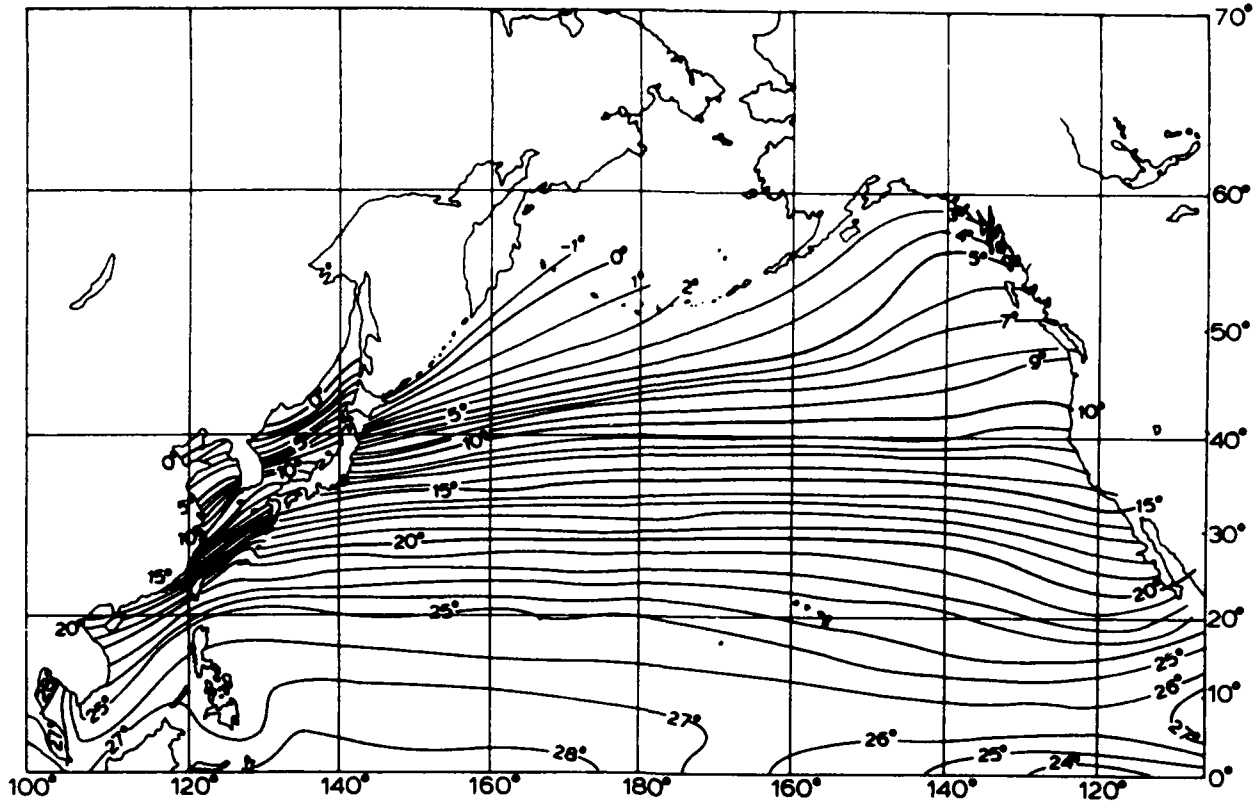


Fig. 23. Sea surface temperature, February.

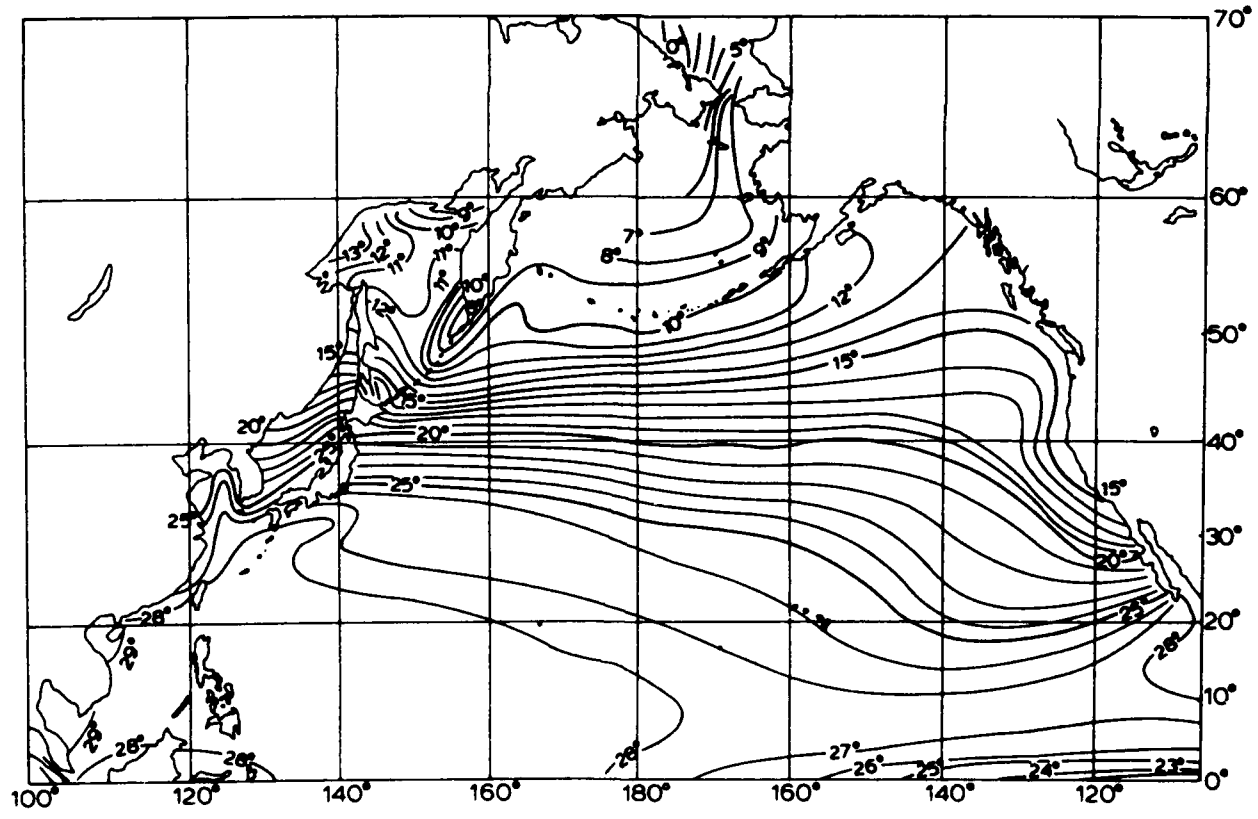


Fig. 24. Sea surface temperature, August.

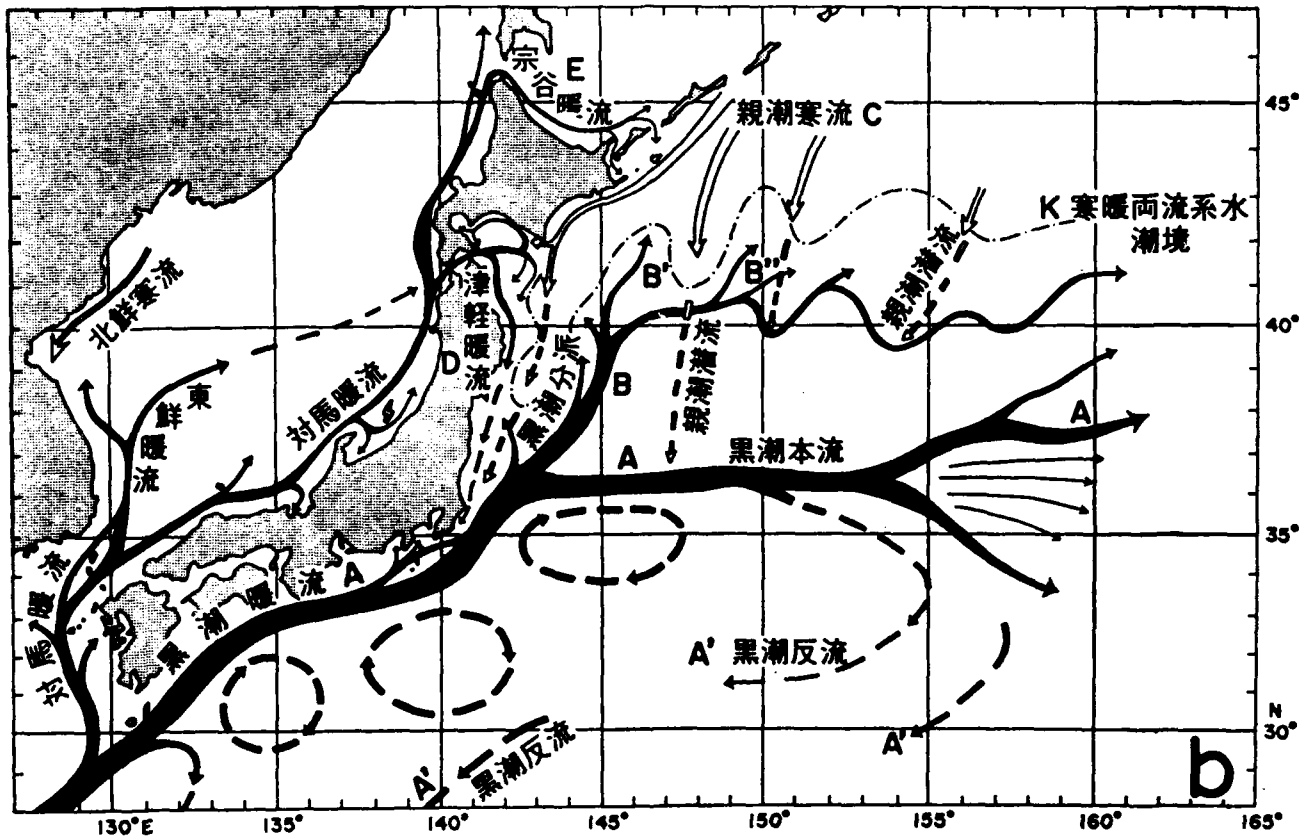


FIG. 6(b) Forklike currents without confluence (Uda, 1935a, Fig. 49b), a schema of the upper structure of currents and waters around the Kuroshio Extension.

Fig. 5

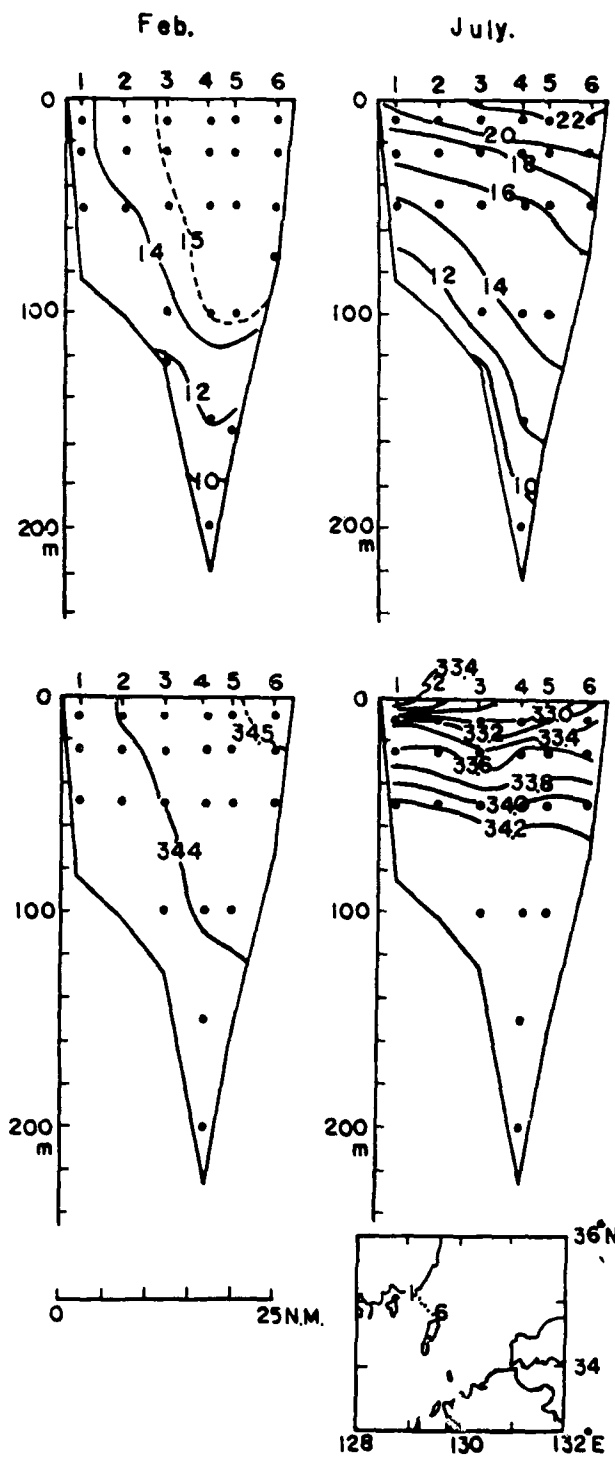


FIG. 8 Vertical sections in the western channel of the Tsushima Strait based on normal values compiled by the Fisheries Research and Development Agency, the Republic of Korea (1964).
Upper temperature in °C; lower salinity in ‰.

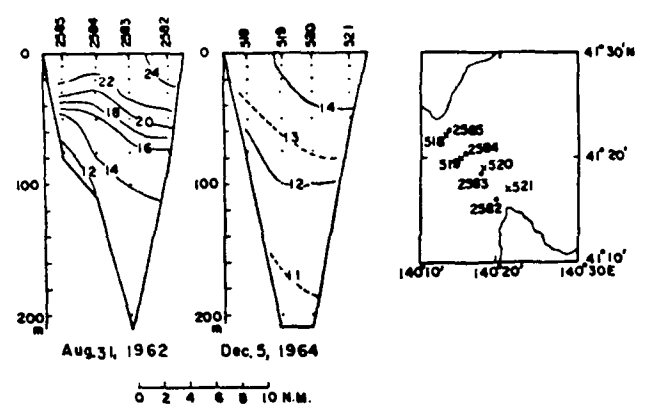


FIG. 9 Vertical sections of temperature (°C) in the Tsugaru Strait. August 31, 1962 voyage of the *Yushio Maru*, December 5, 1964 voyage of the *Kofu Maru*.

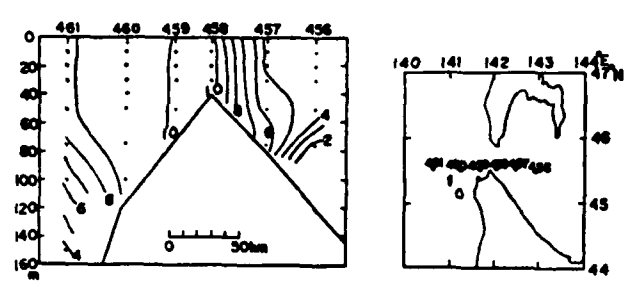


FIG. 10 Vertical section of temperature (°C) around the Soya Strait based on data obtained during a voyage of the *Kofu Maru* in November, 1963.

Fig. 6

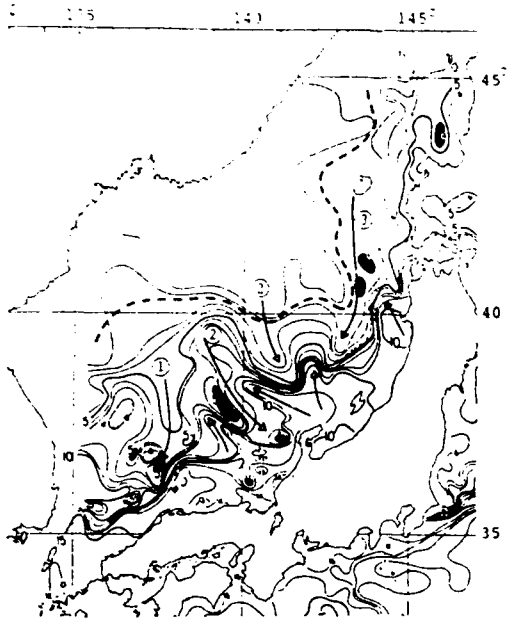


Fig. 1. Isotherms at 100 m depth in May, 1987. Cold and warm intrusions are numbered in order to be traced in June isotherms. Polar front is indicated by a broken line. Cold eddies are shaded. Warm eddies are dotted.

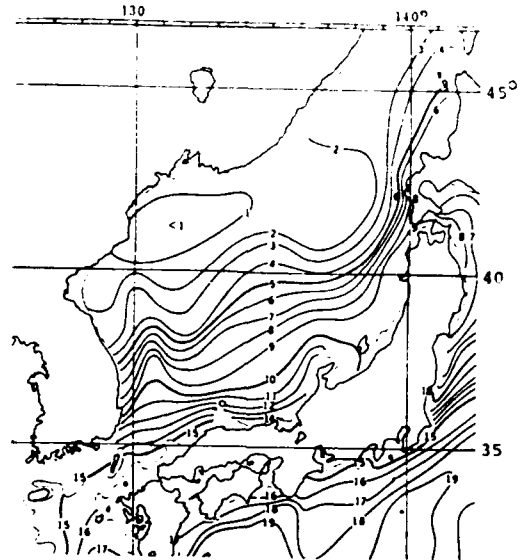


Fig. 3. Isotherms at 100 m from the climatological mean from 1900 to 1972 (JODC, 1978) in May.

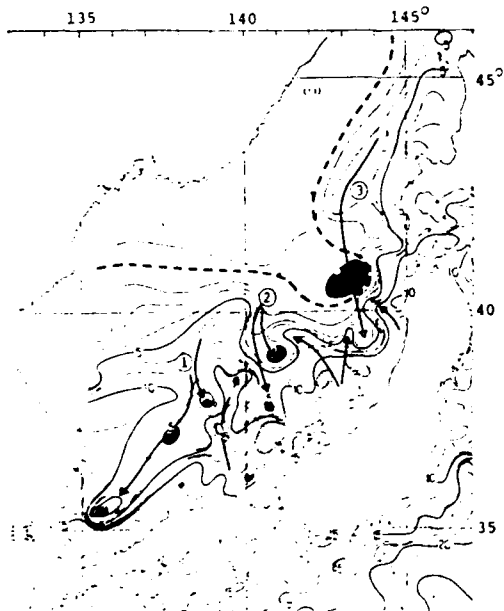


Fig. 2. Isotherms at 100 m depth in June, 1987. See legend of Fig. 1.

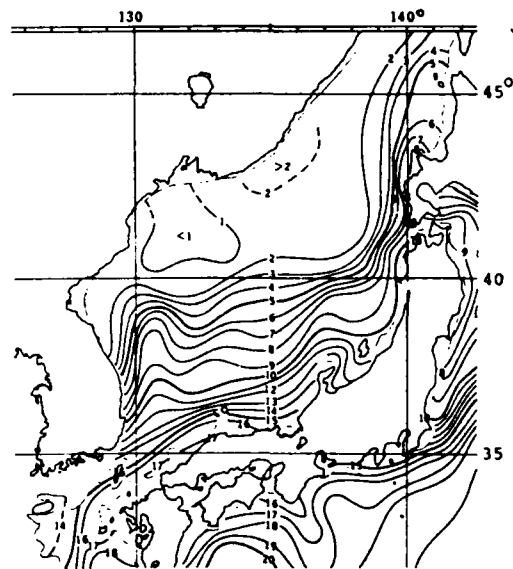


Fig. 4. Isotherms at 100 m from the climatological mean from 1900 to 1972 (JODC, 1978) in June.

Fig. 7

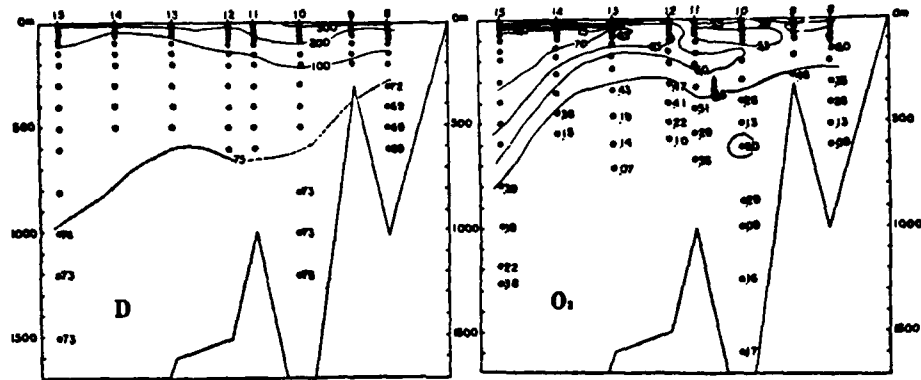
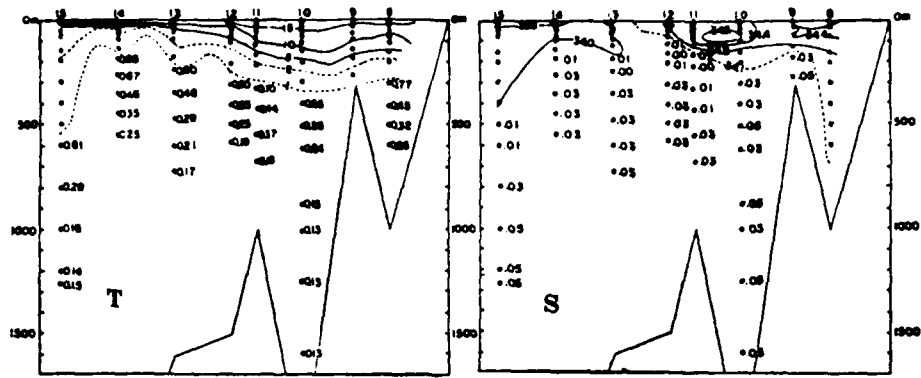


FIG. 4 (1)

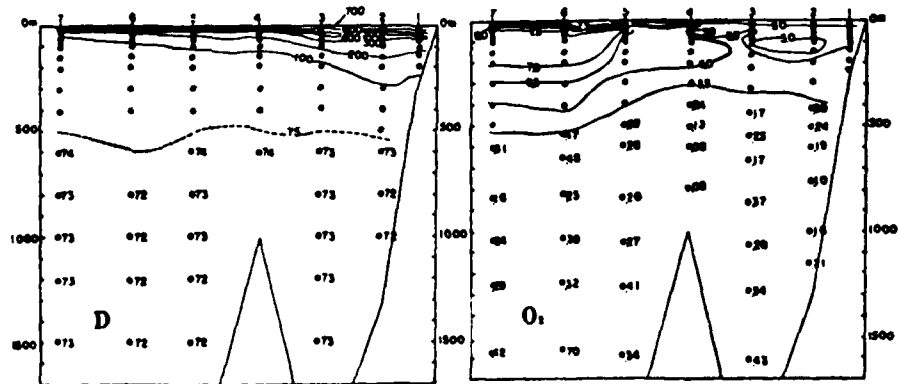
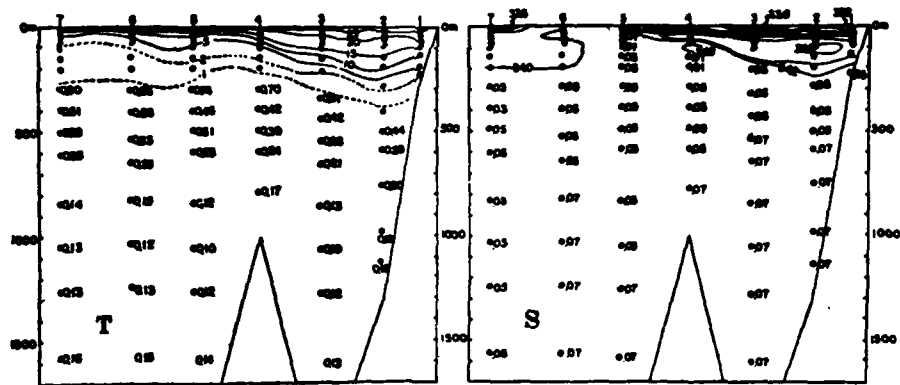


FIG. 4 (2)

Fig. 8a

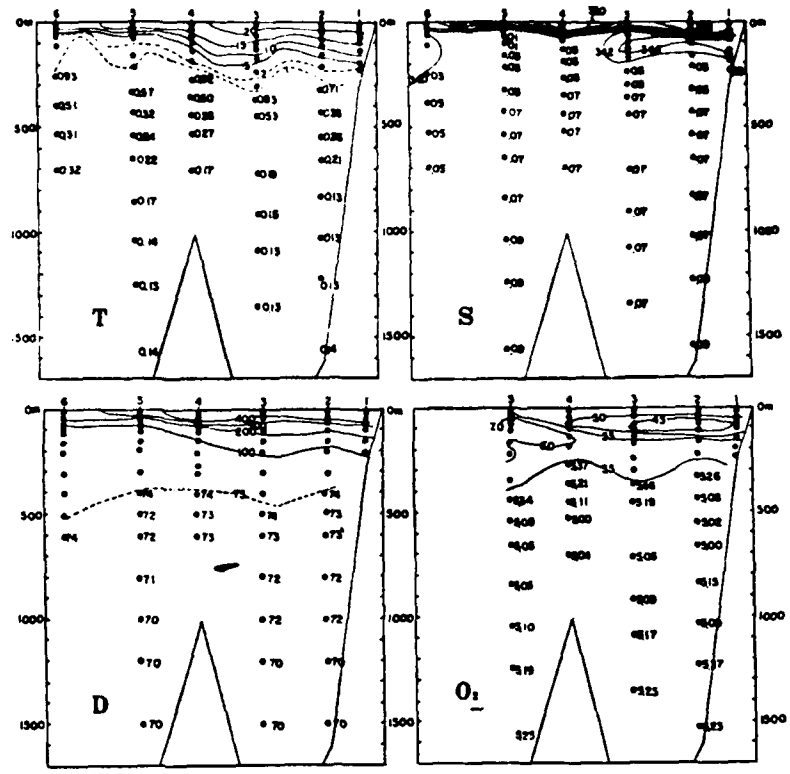


FIG. 4 (3)

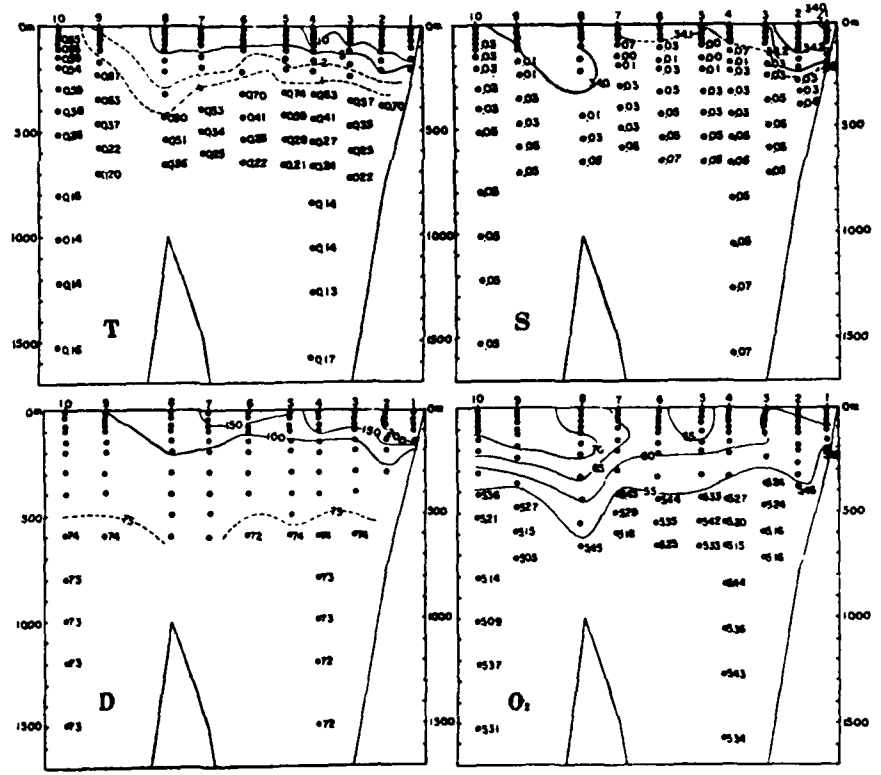


FIG. 4 (4)

FIG. 4 *Seifu Maru* Sections.
 (1) May, 1964; (2) August, 1964;
 (3) October, 1964; (4) February,
 1965; (5) Location of sections.
 T=temperature in °C; S=salinity
 in ‰; D=thermosteric
 anomaly in cl./t; O₂=oxygen
 content in ml./l.

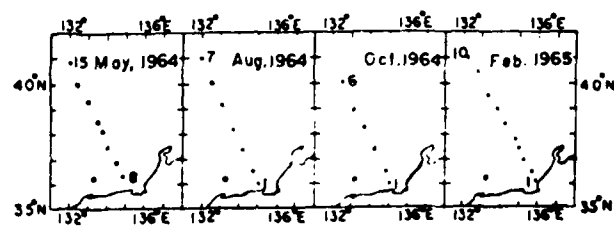


FIG. 4 (5)

Fig. 8b

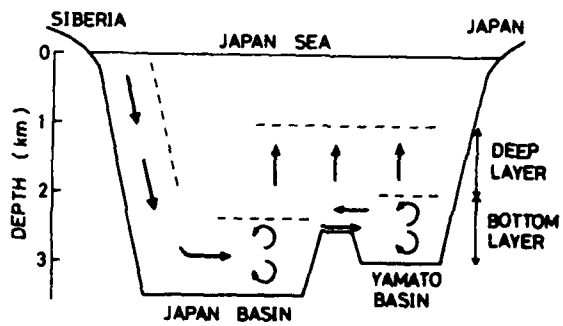


Figure 8. Simplified vertical section of the Japan Sea with a schematic flow pattern of the abyssal circulation. Eddy-like arrows stand for the concept of active vertical mixing, not for real direction of water currents.

Fig. 9

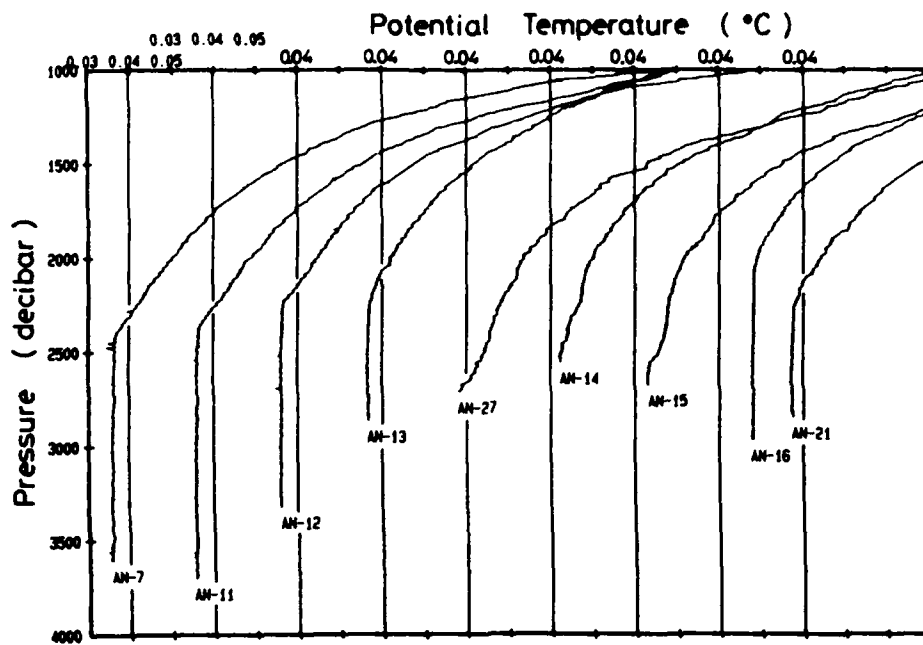


Figure 2. Vertical distributions of CTD potential temperature at stations AN7, 11, 12, 13, 27, 14, 15, 16, and 21. The abscissa is shifted by 0.02°C for every station.

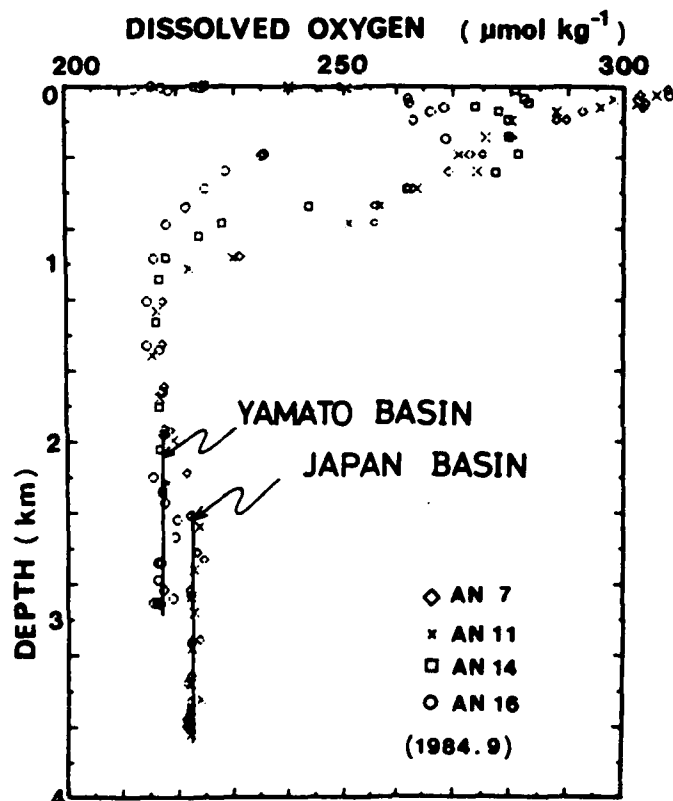


Figure 4. Vertical distribution of dissolved oxygen at stations AN7, 11, 14, and 16.

Fig. 10